

Source-Rock, Reservoir and Hydrocarbon Mapping Using Far-Offset, Elastic Impedance and Extended Elastic Impedance Seismic Volumes, Volve Field, Offshore Norway, North Sea

Khanh Pham Le Huy*

Petroleum Geoscience Program, Department of Geology, Faculty of Science,
Chulalongkorn University, Bangkok 10330, Thailand

*Corresponding author email: khanhplh@gmail.com

Abstract

Mapping formation boundaries and generating the distribution of rock and fluid properties are desirable objectives for reservoir production and further exploration. To achieve the study's objectives, Rock-physics analyses, AVO analyses, Elastic Impedance and Extended Elastic Impedance inversion methods were applied for two main lithologies include sandstone reservoir in Hugin Formation and the potential source rocks - high organic claystone in Draupne Formation. The study shows that the Near-angle stack seismic data and Far stack seismic data would have the best image for the Top Draupne organic-rich claystone (classified as AVO class IV) and the Top Hugin sandstone (classified as AVO class II) respectively. The oil sand within the Hugin Formation and the high organic claystone within the Draupne Formation were identified by applying the inversion based cross-plot method for the Near and Far elastic impedance inversions. The Extended elastic impedance inversion method was applied to generate inversions at specific χ angle to relatively represent Vclay and porosity. Seismic attributes applied for these inversion volumes at Hugin and Draupne Formation provide the distribution of rock-fluid properties and other geology information such as depositional environments. In general, the study indicated the most suitable seismic data for mapping formation boundaries and generated the distribution of rock and fluid properties using seismic inversion methods.

Keywords: AVO Classification, Elastic impedance, Extended elastic impedance, Inversion, Partial-angle stacked seismic

1. Introduction

The study area, Volve field is located in offshore Norway, North Sea. It is in the central part of the North Sea, about 10 kilometers east of Sleipner Vest field. The field is a dome-shaped structure formed by the collapse of adjacent salt ridges during the Jurassic period which gave the field the dome-shaped structure (Szydlik et al., 2007).

The study area is on the Theta Vest structure within the Sleipner Terrace, in the southern Viking Graben, an asymmetric half-graben bounded to the west by the Graben Boundary Fault zone (GBFZ), located along the northern arm of the North Sea rift system (Jackson et al., 2012). The Sleipner Terrane is located to the

west of Utsira High and bounded to the west side by Sleipner Fault - a major boundary fault (Zadeh et al., 2016) (figure 1).

The aim of this study is to test the usefulness of angle-stack data in mapping formation boundaries and generating the distribution of rock and fluid properties in the sandstone reservoir - Hugin Formation and the potential source rock - Draupne Formation. Within the Volve field, two other interesting lithologies are Limestone/marls in Shetland Group and Salt in Zechstein Group (figure 2).

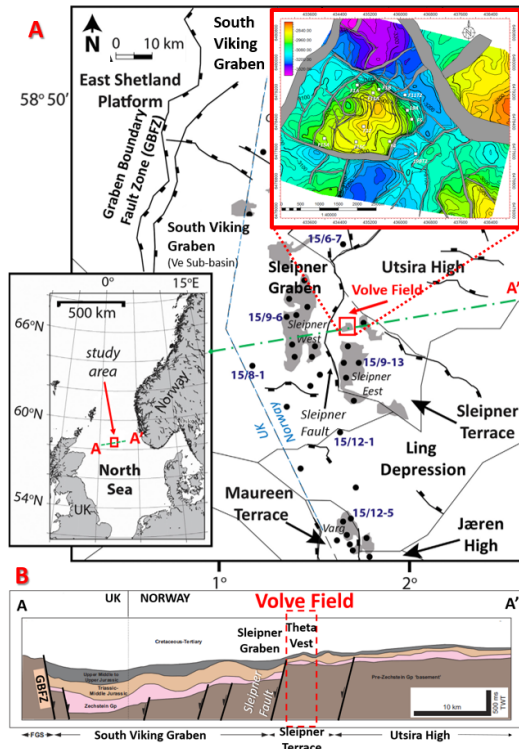


Figure 1: Location of the Volve field. A. showing the geological setting and structural elements (modified from Zadeh et al., 2016). B. The study area – Volve field located on the footwall of South Viking Half-Graben (modified from Jackson et al., 2012).

System	Series	Group/ Supergroup	Formation	Structural and/or tectono-stratigraphic significance
Cretaceous	Upr.	Shetland	Jorsalfare	Post-rift
			Kyrre	
			Tryggvason & Blotekes	
	Lwr.	Cromer Knoll	Svarte	
			Rødby	
Sola				
Asgard				
Jurassic	Upr.	Viking	Draupne	Jurassic minibasin fill
	Mid.	Vestland	Heather	
			Hugin	
Sleipner	Pre-rift			
Triassic		Hegre	Skagerrak	Triassic minibasin fill
Smith Bank	detachment			
Permian	Upr.	Zechstein		

Figure 2: Stratigraphic column of the South Viking Graben – Norwegian sector (modified from Jackson et al., 2010). Red polygons indicate interesting lithologies for the study.

Mapping the boundaries between formations are very essential since the quality of structural maps affect the reservoir volume

estimation or exploration/production planning. Using full-stack seismic data sometimes encounter difficulties in interpreting horizons due to abnormal lithology or fluid effects, which reduce the data resolution, especially within the sandstone reservoir. Due to the AVO effect, which means amplitude change with offset (angle), the same horizon would have higher resolution and amplitude in the angle stack than in the full stack seismic data. Thus, selecting seismic data affect significantly the quality of interpretation results. Besides, for reservoir production and further exploration, generating the distribution of rock and fluid properties are essential objectives which can be achieved by applied seismic inversion method.

Therefore, two specific objectives of this study include selecting the best angle-stack seismic data for mapping and post-stack volume for inversion. For the first objective, the rock physics analysis will be done by using well log data to determine which elastic properties could have the best contrast between different formations, could differentiate between clean sand and shale or could separate the oil sand within the main reservoir interval. Thus, predictions of seismic response based on rock-physics analysis can be made and these predictions will be cross-checked by AVO analysis. The best seismic data for each formation will be selected. The result of the rock physics step will be used for the post-stack inversion. The objective of this step is to invert the seismic reflectivity data into impedance volume by using an integration of well log and seismic data. Two methods include Elastic Impedance inversion and Extended Elastic Impedance Inversion were applied. Using inversion base cross-plot methods and surface attribute of inversions volume, distribution maps of rock and fluid properties will be generated.

2. Methodology

2.1 Rock-physics and AVO analysis

The relationship between petrophysical data and elastic properties were established by analyzing Rock physics of the formation. By

using well log data including P-wave velocity (V_p), S-wave velocity V_s and Density – ρ , the acoustic impedance and near/far-angle elastic impedance were computed by using the following formulas:

- Acoustic Impedance (Aki and Richards, 1980):

$$AI = \rho * V_p \quad (1)$$
- Reflection coefficient (normal incidence) :

$$R = \frac{AI_2 - AI_1}{AI_2 + AI_1} \quad (2)$$
- Elastic Impedance at specific angle θ (Connolly, 1999):

$$EI(\theta) = V_p^a V_s^b \rho^c \quad (3)$$

Where,

$a = 1 + \tan^2(\theta)$, $b = -8K\sin^2(\theta)$, $c = 1 - 4K\sin^2(\theta)$, $K = \frac{V_p^2}{V_s^2}$, ρ : Density; V_p : P-wave velocity; V_s : S-wave velocity, AI_1 and AI_2 : Acoustic impedance of upper and lower layer respectively.

Well base cross plot analysis for lithology and fluid determination were generated to predict seismic response at interested formation boundaries.

Using offset gather seismic data, AVO analysis was applied to cross-check these predictions. According to Amplitude versus Offset (AVO) classification after Rutherford and Williams (1989), extended by Castagna and Smith (1994), and Ross and Kinman (1995), four classes of AVO can be recognized (figure 3). Therefore, we can determine which angle-stack seismic data is better for mapping the interested formation horizons.

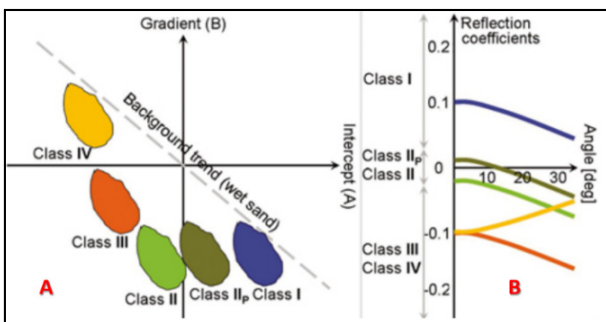


Figure 3: AVO Classification on Cross-plot of A. The intercept versus gradient, B. Reflection coefficient vs. Angle of incidence (CGG, 2019).

2.2 Elastic impedance inversion

Elastic properties are the link between the geology information (well log data) and geophysics information (seismic reflectivity data). The reflectivity data can be calculated from the elastic properties using Shuey’s equation (Shuey, 1985):

$$R(\theta) = R(0) + G\sin^2(\theta) + F\tan^2(\theta) \sin^2(\theta) \quad (4)$$

Where,

$$G = \frac{1}{2} \frac{\Delta V_p}{V_p} - \frac{2V_s^2}{V_s^2} \left(\frac{2\Delta V_s}{V_s} + \frac{\Delta \rho}{\rho} \right),$$

$$F = \frac{1}{2} \frac{\Delta V_p}{V_p},$$

$$R(0) = \frac{1}{2} \left(\frac{\Delta V_p}{V_p} + \frac{\Delta \rho}{\rho} \right).$$

At $\theta=0^\circ$, $R(\theta) = R(0)$ which is the Acoustic impedance, combination of P-wave velocity V_p and density ρ .

In the other way, the Elastic Impedance can be generated from Seismic reflectivity data using Inversion method. This technique requires an initial low-frequency model of elastic impedance computed from the well log data. From the low-frequency model, the seismic reflectivity data was inverted into elastic impedance volume.

The inversion results were QC by blind well test method. The rock-physics results from well-based cross-plots were applied for Inversion-based cross-plots for lithology and fluid determination.

2.3 Extended elastic impedance inversion

Although Elastic impedance inversion is a very useful method, it still has some limitation includes restriction of incident angle (θ) and for different angles (θ), the dimensionality varies and the numerical results do not scale correctly (Whitcombe, 2002). To overcome these difficulties, the extended elastic impedance concept was introduced by Whitcombe et al. (2002). The angle range was extended from $\theta = (0^\circ \text{ to } 30^\circ)$ to $\chi = (-90^\circ \text{ to } +90^\circ)$. The Extended Elastic Impedance equation for specific chi (χ) angle (Whitcombe, et al., 2002):

$$EEI(\chi) = V_{p0}\rho_0 \left[\left(\frac{V_p}{V_{p0}} \right)^{(\cos \chi + \sin \chi)} \left(\frac{V_s}{V_{s0}} \right)^{(-8k \sin \chi)} \left(\frac{\rho}{\rho_0} \right)^{(\cos \chi - 4k \sin \chi)} \right] \quad (5)$$

$$EEI(\chi) = AI^{\cos \chi} GI^{\sin \chi} \quad (6)$$

Where,

χ : project angle

$$K = \frac{Vp^2}{Vs^2}$$

V_{p0} , V_{s0} and ρ_0 : Normalization constants of P-wave velocity, S-wave velocity and density; AI & GI: Intercept and Gradient

From the well data, the EEI was computed from V_p , V_s and ρ with χ (χ) angle ranges from -90° to 90° . The results were cross correlated with \emptyset , V_{sh} & S_w to optimize the best χ (χ) angles for those properties. The EEI Reflectivity volumes at best χ (χ) angles were generated from AI as GI. Inversion of these volumes could relatively represent rock properties: \emptyset , V_{sh} , S_w . Surface attribute method was applied to inversion results to generate the relative lithology and fluid properties distribution.

3. RESULTS AND INTERPRETATION

3.1 Rock-physics

The well log, impedance properties and seismic response prediction of these formation boundaries were summarized in figure 4 and table 1.

In general, due to the high contrast in Density and Sonic values, Top of Limestone on Shetland Group and Salt in Zechstein Group have high contrast on both AI, Near and Far EI. They would be high positive amplitude reflectors (peak) on all seismic data and their amplitude would decrease with angle (the near-angle stack data have higher amplitude than the far one).

The Top Draupne Formation in the Near EI has the best contrast at the boundaries while the Far EI has the best contrast at the boundaries of the Hugin sandstone. Therefore, the near stack seismic data and far stack seismic data would have the best image for the Top Draupne organic-rich claystone and the Hugin sandstone respectively.

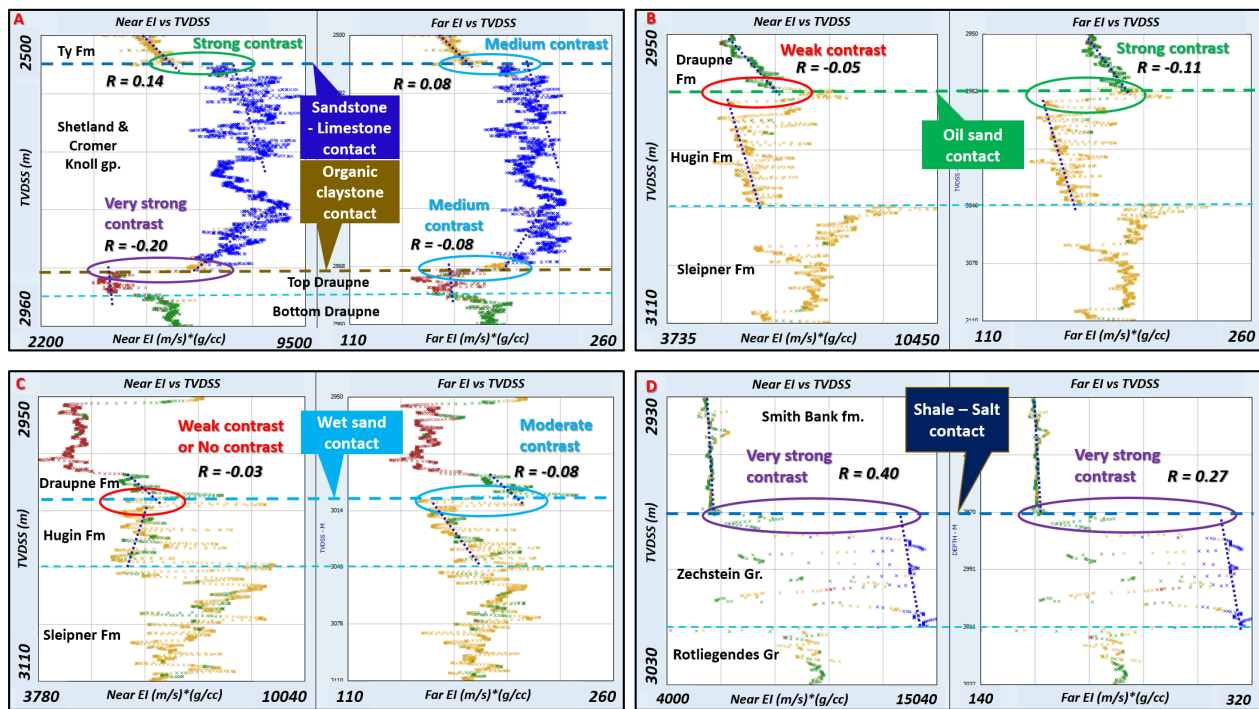


Figure 4: Depth (x-axis) vs. AI & Near/Far EI (y-axis) against clay volume (Vclay) in A. Shetland Limestone and Top Draupne high organic claystone; B. Oil sand in Hugin Formation; C. Wet sand in Hugin Formation; D. Salt formation - Zechstein Group.

Table 1: Well logs and Acoustic/Elastic Impedance at Formation boundaries

Formation	Well log signatures at the top	Acoustic Impedance (AI)	Near Elastic Impedance (EI)	Far Elastic Impedance (EI)	Seismic Response Prediction
Limestone/marl - Shetland Group	Increase: Density Decrease: GR, DT, Neutron	Strong positive contrast. R = 0.12	Strong positive contrast. R = 0.14	Medium positive contrast. R = 0.08	High positive amplitude reflector on all seismic data, and decreases with angle.
High organic claystone - Top Draupne Formation	Increase: GR, DT, Neutron Decrease: Density	Very strong negative contrast. R = -0.20	Very strong negative contrast. R = -0.20	Medium negative contrast. R = -0.08	High negative amplitude reflector (trough) on Near stack data. Lower amplitude trough on Far stack data.
Oil Reservoir sandstone - Hugin Formation	Increase: Resistivity Decrease: GR, DT, Density	Weak negative contrast. R = -0.05	Weak negative contrast. R = -0.05	Strong negative contrast. R = -0.11	Low negative amplitude reflector on Near stack data. Stronger negative amplitude reflector on Far stack data.
Wet Reservoir sandstone - Hugin Formation	Increase: N/A Decrease: GR, DT, Density	No or very weak negative contrast. R = -0.02	No or very weak negative contrast. R = -0.03	Moderate negative contrast. R = -0.08	Very low negative amplitude or Zero crossing on Near stack data. Moderate-Weak negative amplitude reflector on Far stack data.
Salt formation - Zechstein Group	Increase: Density, & Resistivity Decrease: GR & DT	Very strong positive contrast. R = 0.40	Very strong positive contrast. R = 0.40	Very strong positive contrast. R = 0.27	High positive amplitude reflector on all seismic data. Amplitude decreases with angle.

3.2 AVO analysis

The above prediction was tested by doing seismic well-tie and AVO analysis. The results show that all predictions are a good match with the actual seismic response. In general, the top of Limestone/marl formation-Shetland Group and Salt formation- Zechstein Group are high positive amplitude reflectors (peak) on all seismic data and classified as AVO Class I.

The top of organic-rich claystone in Top Draupne is negative amplitude reflector (trough) and the reflector in the near stack data have higher amplitude and continuity than those in the far stack, which is AVO Class IV. The Hugin sandstone formation top was imaged as a trough (negative) and when compared to near stack data, the reflector in the far stack data have higher amplitude and continuity, which is AVO class II (figure 5 and 6).

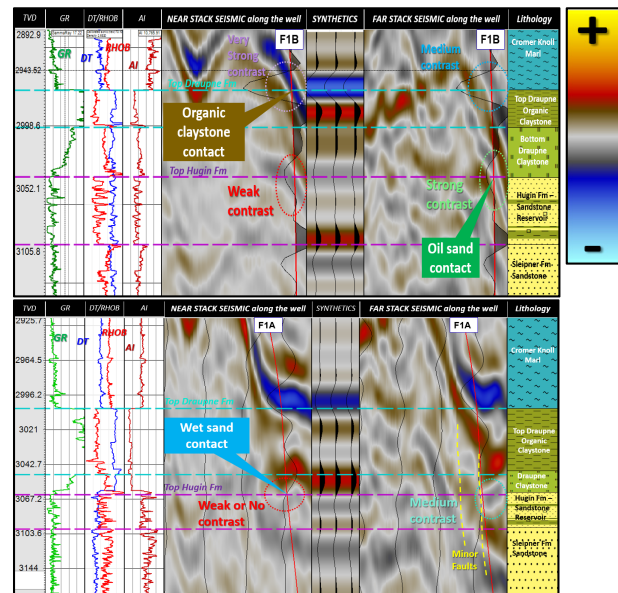


Figure 5: Seismic synthetics and actual near/far stack seismic data along the Oil well 15/9-F1B (Top) and Wet well 15/9-F1A (Bottom).

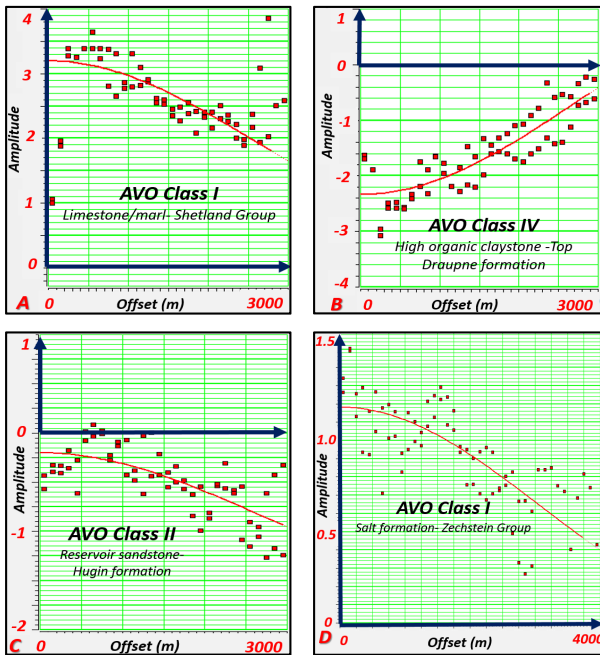


Figure 6: AVO Analysis results for A. Top Limestone – Shetland Group, B. Top high organic claystone – Draupne Formation, C. Top reservoir sandstone -Hugin Formation, D. Top Salt formation – Zechstein Group.

3.3 Elastic impedance inversion

Five important steps in post-stack inversion include Wavelet extraction, Seismic-well tie, Low frequency modeling, Inversion analysis and Inversion generation. Wavelets were extracted statistically using both seismic and well data. By using these wavelets, the seismic synthetic of each well was generated and the seismic-well ties were done to calibrate checkshot data and correlate all wells. The correlation coefficients of each well are generally good since they range from 0.7 to 0.9. Since the seismic is band-limited, low frequency information (0-5 Hz) information is missing. Therefore, low frequency model generated from well log data is very important for the inversion study. Four main horizons were used for modeling include Top Shetland Group, Top Draupne Formation, Top Hugin Formation, Top Sleipner formation (Hugin Base). Two models using near and far elastic impedance from well data were generated for near and far elastic impedance inversion. Inversion Analysis was done to test the inversion parameters before actual application by calculating the correlation coefficient between the inversion elastic

impedance against the computed one from well data. The analysis shows that at all wells, the correlation coefficient is generally good since it ranges from 0.8 to 0.9. A blind-well test was applied to show the quality of inversion results. Since the colored inversion showed better results in all area when comparing to the model-based inversion, the colored inversion method was chosen for further application. The results of Near and Far elastic impedance inversion generated by the colored inversion method were shown in figure 7.

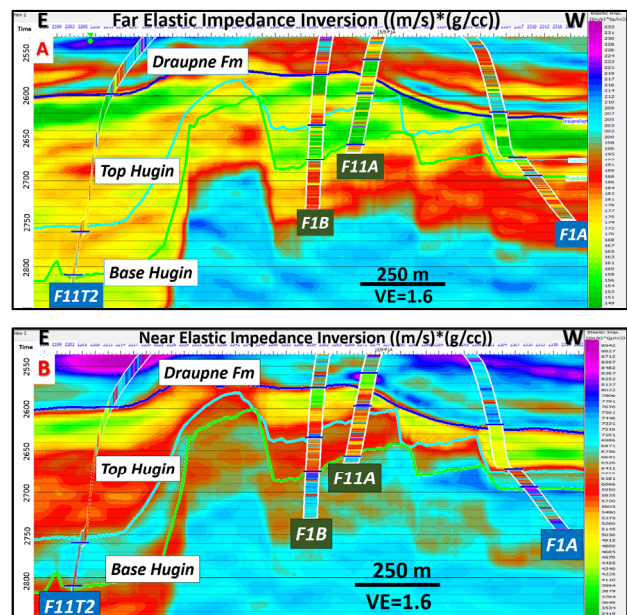


Figure 7: Elastic inversion results. A. Far Elastic Impedance Inversion; B. Near Elastic Impedance Inversion (blind well test at F1B – Display on Xline 10211).

On well log data, by cross plotting the computed Near EI and Far EI (as x-y axis) against Water saturation or Vclay (as color), the oil zone can be identified from the wet zone and high organic zone can be identified from other zones. Polygons that defined oil zone and high organic zone on well-log cross-plot were applied on the inversion cross-plot between Near and Far EI inversion. The display of the zones on seismic for the data within the polygons can be used to predict the distribution of oil sand in the Hugin formation and source rock – high organic claystone in the Draupne formation (figure 8).

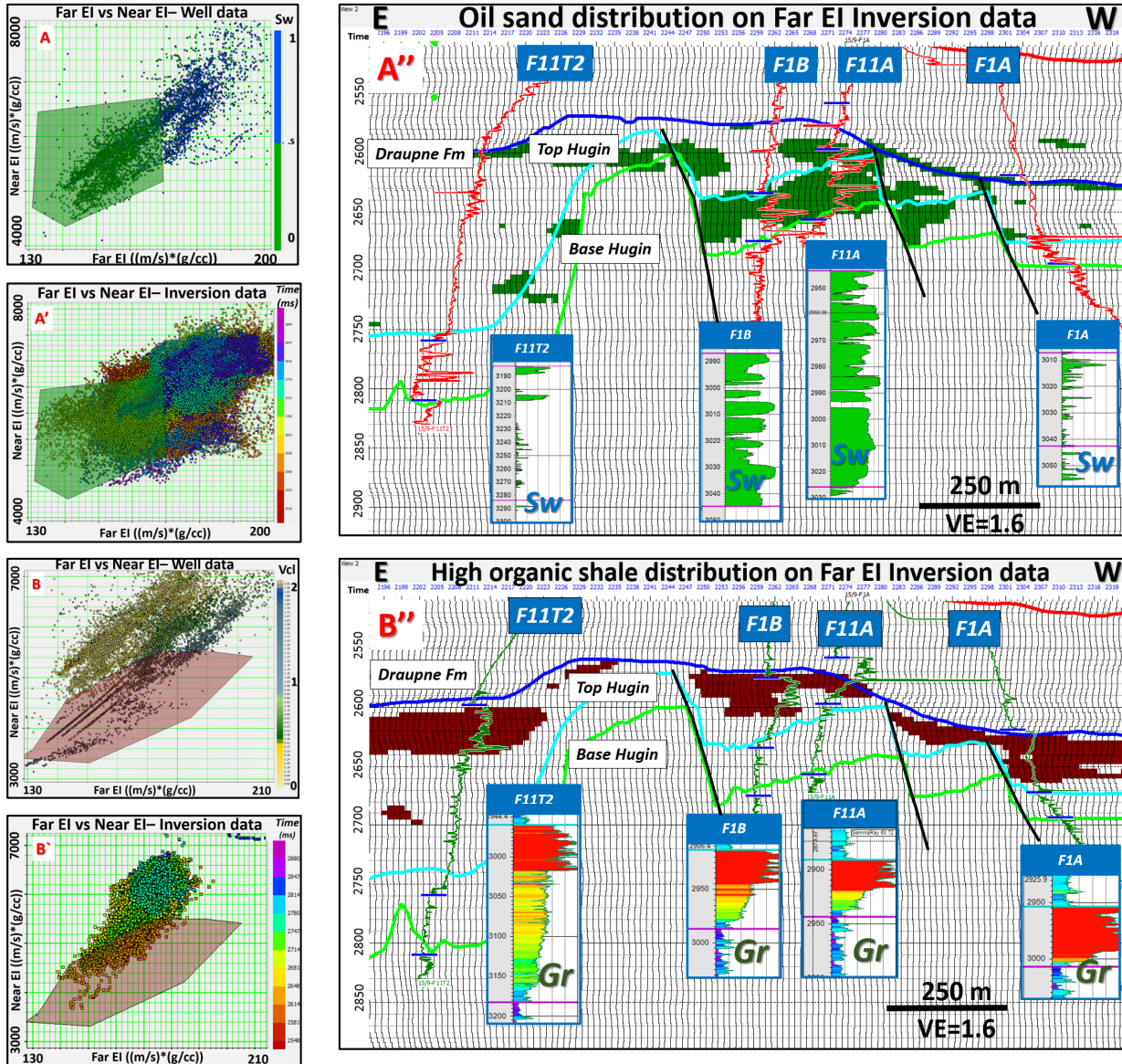


Figure 8: Oil sand distribution in Hugin Formation and High organic claystone distribution in Draupne Formation. A/B. Near and Far EI well data crossplot - The green/brown polygon defined the oil/high organic zone; A'/B'. Near and Far EI inversion data crossplot - The green/brown polygon from well cross-plot; A''/B''. Oil sand/High organic claystone distribution- green/brown color represents oil sand/high organic zones (Resistivity log/Vclay was plot along wells and Sw/Gr results were displayed to crosscheck).

3.4 Extended elastic impedance inversion

The first and the most important step in Extended elastic impedance Inversion is optimizing chi (χ) angle. The process shows that: Vclay and porosity (\emptyset) show good correlation with EEI ($\chi = 51^\circ$) and EEI ($\chi = 6^\circ$) respectively. However, Sw show low

correlation with EEI and the χ angle varied in a wide range of value. Therefore, EEI Inversion would represent Vclay and \emptyset value, but is not useful for Sw. From the previous step result, the EEI Reflectivity volumes and EEI well-log at chi (χ) angle 51° and 6° were computed (figure 9).

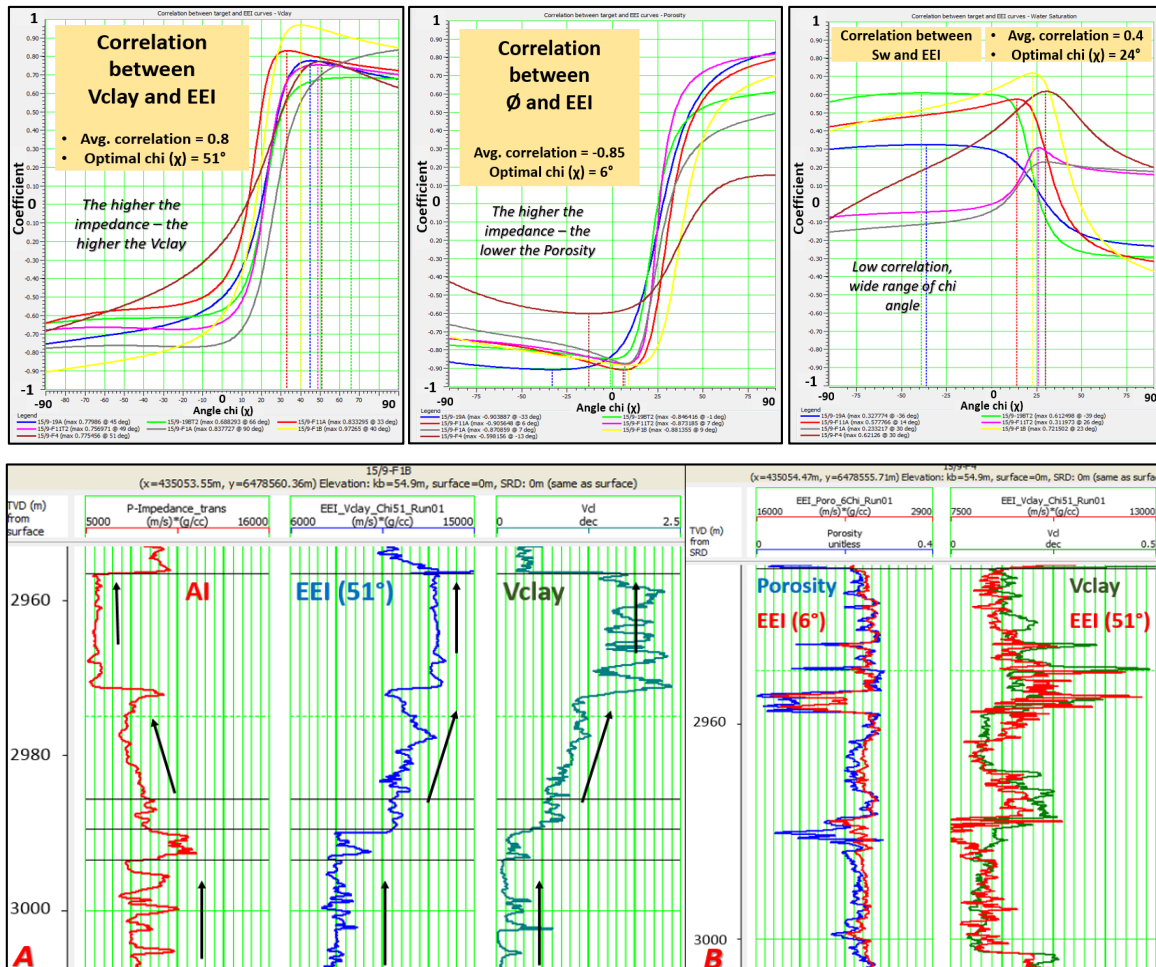


Figure 9: Optimizing chi (χ) angle results and Computed EEI well log at chi (χ) angles 51° and 6° compared with Vclay and porosity log. A. The advantage of using EEI in relatively representing Vclay properties, comparing to AI; B. EEI (6°) and EEI (51°) relatively represent Porosity and Vclay respectively.

Using the same method in the elastic impedance inversion, the EEI inversion at chi (χ) angles 51° and 6° were then generated. Since the correlation coefficient between EEI Inversion at $\chi=51^\circ$ and Vclay is 0.8 (high positive value), the higher the amplitude of the inversion the higher the Vclay value. In a reverse way, since the correlation coefficient between EEI Inversion at $\chi=6^\circ$ and Vclay is -0.85 (high negative value), the higher the amplitude of the inversion the lower the porosity value. The RMS surface attribute was applied to the inversion volume to generate the distribution map of Vclay and \emptyset at interested zones.

Since this method does not give the absolute value of Vclay or porosity, these attribute maps only relatively represent the distribution of Vclay or porosity. Results were combined in figure 10 and 11, property values at each well

were plotted on the same attribute map as a crosscheck.

On figure 10 – The Hugin Formation, the red polygon defines the oil zone within the high structures, where most wells are located. The relative porosity map (figure 10C) show that the porosity increases toward the Southeast. The relative Vclay map (figure 10D) shows that Vclay decreases toward the Southeast. Since the Hugin Formation was deposited in a mouth-bar setting – shallow marine environment (Statoil, 1993), the porosity and Vclay trend would indicate that the clastic material was carried and deposited from the Southeast (High porosity – low Vclay) to the Northwest (Low porosity – High Vclay). Within the oil zone, the eastern side with greater thickness, higher porosity and lower Vclay value is a good place for further production. There is a possible structure toward

the Southeast with low V_{clay} and high porosity. However, due to limited data, the possibility is unclear.

On figure 11 – The Draupne Formation, the relative V_{clay} map shows the distribution of the high organic claystone – source rock. The high organic claystone is not equally distributed

across the area. It is thinner in the high structure area and become thicker in the low structure area. Since this formation was deposited in a marine environment with restricted bottom circulation (Statoil, 1993), the pre-existing structure may have affected significantly the V_{clay} distribution.

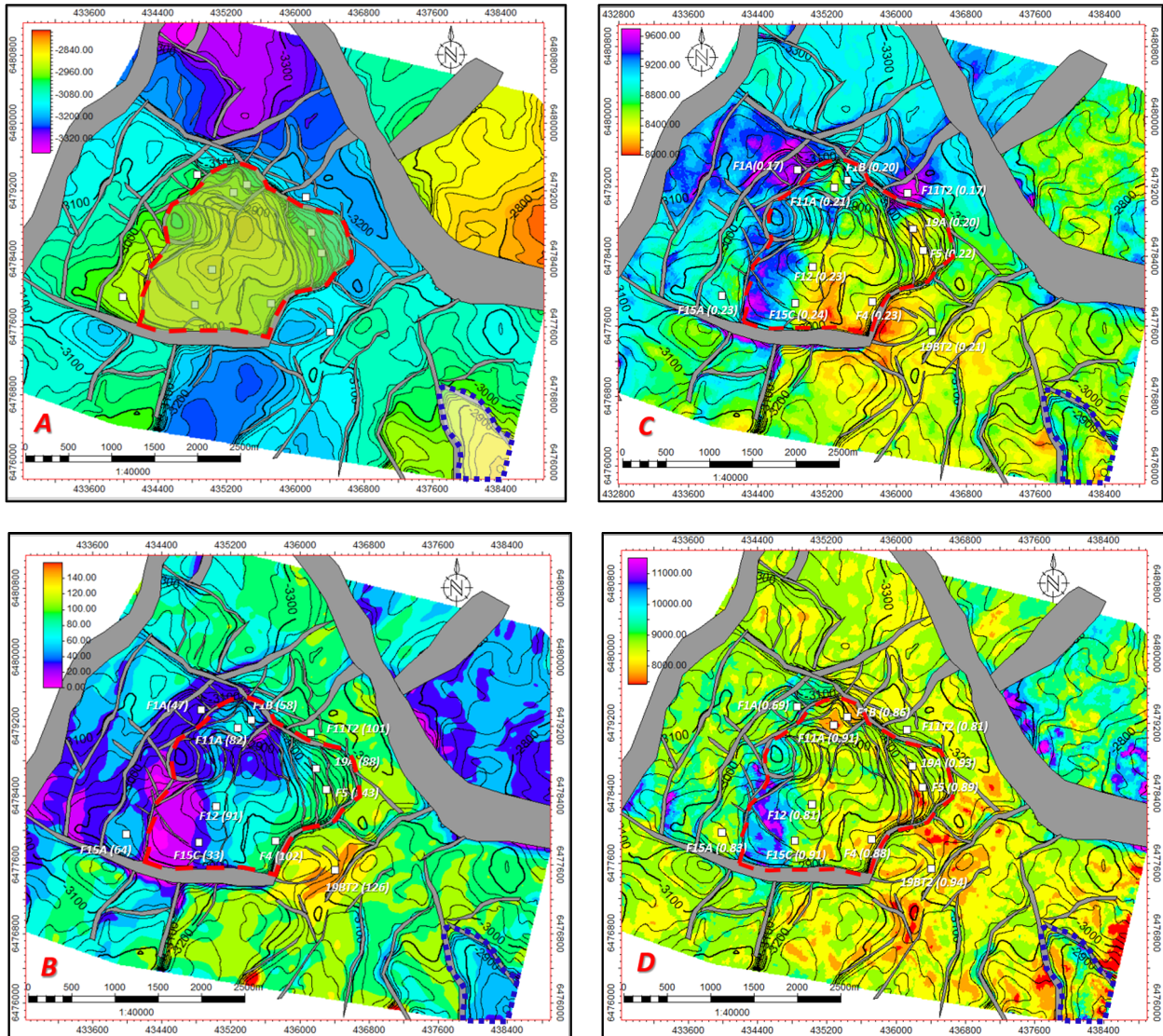


Figure 10: Relative V_{clay} and Porosity distribution map of Hugin Formation. A. Depth structural map , B. Isochore (thickness) map – The hotter the color (red-yellow), the greater the thickness, C. EEI Inversion ($\chi=6^\circ$) surface attribute map – relative porosity distribution map (The hotter the color – yellow and red, the lower the EEI, the higher the porosity), D. EEI Inversion ($\chi=51^\circ$) surface attribute map – relative V_{clay} distribution map (The hotter the color, the lower the EEI, the lower the V_{clay}). The red and blue polygon define the oil zone and the potential structure respectively.

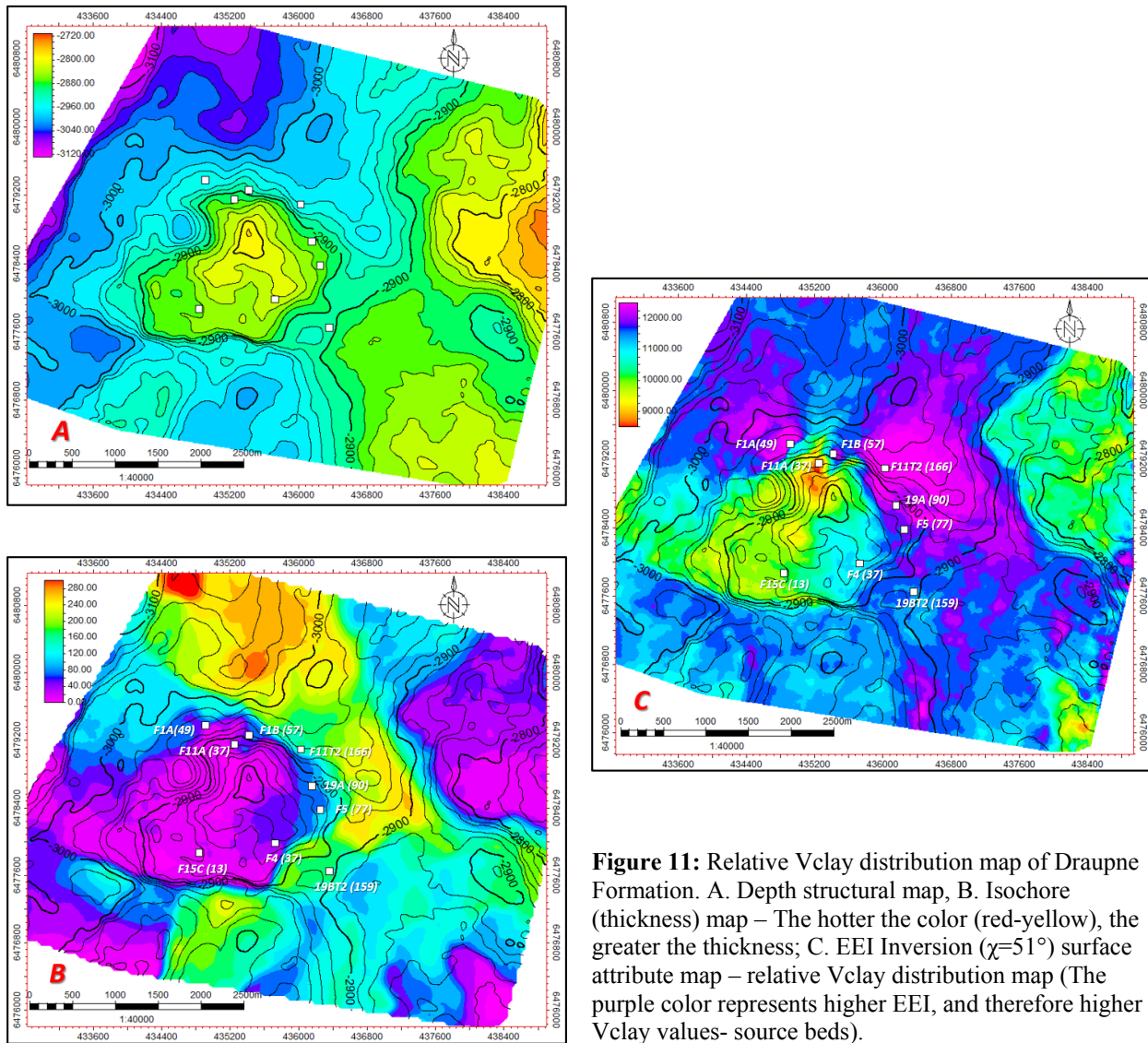


Figure 11: Relative Vclay distribution map of Draupne Formation. A. Depth structural map, B. Isochore (thickness) map – The hotter the color (red-yellow), the greater the thickness; C. EEI Inversion ($\chi=51^\circ$) surface attribute map – relative Vclay distribution map (The purple color represents higher EEI, and therefore higher Vclay values- source beds).

4. Regional application discussion

Besides the study results, there are some interesting points that need to be considered before applying this study method to other areas.

- Rock-physics study can predict correctly how seismic would respond at formation boundaries. In the study area, two conditions that support this method are the great thickness of each formation and the great differences of elastic properties (density and velocity) between two adjacent formations. In this case, the study lithology consists of a thick layer of Carbonate, Organic claystone, Stack sandstone and Salt. This method may not be useful for areas with thin reservoirs (lower than the seismic resolution) or interbedded formations.

- The inversion study included a blind well test. All wells in the study area are located within the small oil production area (7 km²), and all wells are close to each other with distances between wells range from 300 to 1000 meter. This could be a reason for good blind-test results. Since there are no available wells outside the production area to be tested, the result is questionable outside the production area.

- This study shows that Extended elastic impedance inversion method can relatively represent Vclay and porosity. However, this method wasn't useful for Water saturation. The oil in the study area is medium oil with a specific gravity at 15° between 0.88-0.9 g/cc (ResLab,

2008 and Statoil, 1997). This oil specific gravity is close to water specific gravity (1 g/cc). This makes the acoustic impedance of wet sand close to the oil sand, so this method cannot differentiate oil sand from wet sand effectively.

- In Cuulong basin (Vietnam), the sandstone reservoirs in the Lower Miocene is at the same depth with the Hugin Formation in the study area (2700-3000 meters) with the similar porosity (0.15-0.25). However, the Cuulong reservoirs are interbedded sandstone, with a total net reservoir that can achieve 100 meters but the net sand reservoir thickness is smaller than 10 meters. This characteristic is significantly different from Hugin Formation with thick stack sandstone, deposited in a mouth-bar setting - shallow marine environment. Interbedded sand with thin layers (lower than seismic resolution) could create the thin-bed tuning effect which harms real signal amplitude. Since our inversion method quality depended significantly on seismic amplitude, the Cuulong basin reservoir must account for the thin-bed tuning problem before applying the method. The Oligocene source rock in Cuulong basin and the source rock in Draupne Formation have similar lithology (high organic claystone) with a great thickness. Therefore, the study method can be applied to map the distribution of source bed in Cuulong basin.

5. Conclusions

The study in Volve Field, Offshore Norway, North Sea was completed using rock physics analysis, AVO analysis, elastic and extended elastic impedance inversion. The main study objective was mapping the distribution of reservoir and hydrocarbon in the Hugin Formation. Another objective was mapping the distribution of the potential source rock in Draupne Formation. The conclusions are summarized below:

- From the well-logs and rock-physics analysis, Top of Limestone in Shetland Group and Salt in Zechstein Group have high contrast on both Near and Far Elastic Impedance (EI). The Top Draupne Formation in the Near EI has the best contrast at the boundaries while the Far

EI has the best contrast at the boundaries of the Hugin sandstone.

- The AVO analysis showed that the seismic responses predicted from rock-physics analysis match with the seismic data. The top of Limestone in Shetland Group and Salt formation- Zechstein Group are high positive amplitude reflectors (peak) with AVO Type I. The top of organic-rich claystone in Top Draupne is a negative amplitude reflector (trough) with AVO type IV. The Hugin sandstone formation top was imaged as a negative amplitude reflector (trough) with AVO type II.

- The Near and Far Elastic Impedance Post-Stack Inversions were completed on the Hugin Formation (reservoir) and the Draupne Formation (source rock). Cross-plots between Near EI and Far EI inversion were generated and analyzed to identify the oil sand zone within Hugin Formation and the high organic claystone within the Draupne Formation.

- The extended elastic impedance (EEI) inversion method was applied to represent the rock and fluid properties (V_{clay}, Porosity and water saturation). The result showed that the EEI inversion ($\chi=51^\circ$) and EEI inversion ($\chi=6^\circ$) respectively can relatively represent the V_{clay} and porosity. The higher the amplitude of the EEI ($\chi=51^\circ$) inversion the higher the V_{clay} and the higher the amplitude of the EEI ($\chi=6^\circ$) inversion the lower the porosity value. However, this method cannot represent the water saturation since the specific gravity of oil is quite close to that of water. Distribution maps of V_{clay} and porosity can be generated by surface attribute of the inversion volumes.

6. Acknowledgment

I would like to express my sincere gratitude to my thesis supervisor, Professor Angus John Ferguson for his patient guidance, constant help and useful critiques of this study work. I would also like to thank Professor John Keith Warren and Professor Thasinee Charoentitirat for their knowledge and supports through the Petroleum Geoscience Program. I also place on record, my sincere gratitude to Equinor Company for providing the necessary data for this study.

7. References

- Aki, K., and P. G. Richards, 1980, *Qualitative Seismology*, vol. 1, W. H. Freeman, New York.
- Castagna, J.P., and Smith, S.W., 1994, Comparison of AVO indicators: A modelling study, *Geophysics*, 59, p. 1849-1855.
- CGG, 2019, AVO Attribute Extraction: <<https://www.cgg.com/en/What-We-Do/GeoSoftware/Platform-Environment/AVO-Attribute-Extraction>> (accessed June 22, 2019).
- Connolly, P., 1999, Elastic impedance. *The Leading Edge*, 18, p. 438-452.
- Jackson, C. A.-L., K. E. Kane, and E. Larsen, 2010, Structural evolution of mini basins on the Utsira High, northern North Sea; implications for Jurassic sediment dispersal and reservoir distribution: *Petroleum Geoscience*, v. 16, no. 2, p. 105–120, doi:10.1144/1354-079309-011.
- Jackson, Christopher & Kane, Karla & Larsen, Eirik & Evrard, Elisabeth & Elliott, Gavin & Gawthorpe, Rob, 2012, Variability in Syn-Rift Structural Style Associated with a Mobile Substrate and Implications for Trap Definition and Reservoir Distribution in Extensional Basins: A Subsurface Case Study from the South Viking Graben, Offshore Norway: *AAPG Search and Discovery*, 10423.
- Ross, C.P. and Kinman, D.L., 1995, Nonbright-spot AVO: Two examples, *Geophysics*, 60, p. 1398-1408.
- Rutherford, S. R., and R. H. Williams, 1989, Amplitude versus offset variations in gas sands: *Geophysics*, 54, p. 680-688.
- ResLab, 2008, Final Report – PVT analysis of MDT oil samples from well 15/9-f-4, Volve, Project No. 70-517, Report No. 70-00286.
- Shuey, R. T., 1985, A simplification of the Zoeppritz equations: *Geophysics*, 50, P. 609-614.
- Statoil, 1993, Discovery evaluation report – Well 15/9-19 SR – Theta Vest Structure – PL046A
- Statoil, 1997, 15/9-19A, PVT analysis of single phase sample, Report No. STAT550B.
- Szydlak, T. J., S. Way, P. Smith, L. Aamodt, and C. Friedrich, 2006, 3D PP/PS Prestack Depth Migration on the Volve Field: 68th EAGE Conference and Exhibition incorporating SPE EUROPEC 2006, doi:10.3997/2214-4609.201402177.
- Whitcombe, D., 2002, Elastic impedance normalization. *Geophysics*, 67, p. 60-62.
- Whitcombe, D. N., Connolly, P. A., Reagan, R. L., Redshaw, T. C., 2002, Extended elastic impedance for fluid and lithology prediction: *Geophysics*, 67, p. 63-67.
- Zadeh, M. K., N. H. Mondol, and J. Jahren, 2016, Compaction and rock properties of Mesozoic and Cenozoic mudstones and shales, northern North Sea: *Marine and Petroleum Geology*, v. 76, p. 344–361, doi:10.1016/j.marpetgeo.2016.05.024.